Available online at www.sciencedirect.com
ScienceDirect
Geochimica et Cosmochimica Acta 73 (2009) 1890–1900
Geochimica et Cosmochimica Acta
www.elsevier.com/locate/gca

Re-evaluating boron speciation in biogenic calcite and aragonite using ^{11}B MAS NMR

Kateryna Klochko [a,*], George D. Cody [b], John A. Tossell [c], Przemyslaw Dera [b], Alan J. Kaufman [a,d]

[a] Department of Geology, University of Maryland, College Park, MD 20742, USA
[b] Geophysical Laboratory, Carnegie Institution of Washington, Washington, DC 20015, USA
[c] Department of Chemistry and Biochemistry, University of Maryland, College Park, MD 20742, USA
[d] ESSIC, University of Maryland, College Park, MD 20742, USA

Received 28 January 2008; accepted in revised form 5 January 2009; available online 22 January 2009

Abstract

Understanding the partitioning of aqueous boron species into marine carbonates is critical for constraining the boron isotope system for use as a marine pH proxy. Previous studies have assumed that boron was incorporated into carbonate through the preferential uptake of tetrahedral borate $B(OH)_4^-$. In this study we revisit this assumption through a detailed solid state ^{11}B magic angle spinning (MAS) nuclear magnetic resonance (NMR) spectroscopic study of boron speciation in biogenic and hydrothermal carbonates. Our new results contrast with those of the only previous NMR study of carbonates insofar as we observe both trigonal and tetrahedral coordinated boron in almost equal abundances in our biogenic calcite and aragonite samples. In addition, we observe no strict dependency of boron coordination on carbonate crystal structure. These NMR observations coupled with our earlier re-evaluation of the magnitude of boron isotope fractionation between aqueous species suggest that controls on boron isotope composition in marine carbonates, and hence the pH proxy, are more complex that previously suggested.

1. INTRODUCTION

Insofar as aqueous boron species are isotopically distinct, their incorporation into marine carbonates is important to our understanding of the boron isotope system as a proxy for ancient ocean pH. Boron speciation in aqueous solution is well established (Dickson, 1990) with the equilibrium distribution of boric acid [$B(OH)_3$] and borate ion [$B(OH)_4^-$] being strongly pH dependent:

$$B(OH)_3 + H_2O \Longleftrightarrow B(OH)_4^- + H^+. \quad (1)$$

The stoichiometric equilibrium constant for reaction (1) is a function of salinity, temperature and pressure. At a salinity of 35, 25 °C and 1 atm total pressure, $pK^*_B = 8.597$ on the total proton concentration scale (Dickson, 1990).

The isotopic equilibrium between these two species in aqueous solution is characterized by the exchange reaction:

$$^{10}B(OH)_3 + {}^{11}B(OH)_4^- \Longleftrightarrow {}^{11}B(OH)_3 + {}^{10}B(OH)_4^-. \quad (2)$$

Paleo-pH studies of marine carbonates (Vengosh et al., 1991; Hemming and Hanson, 1992; Spivack et al., 1993; Gillardet and Allègre, 1995; Sanyal et al., 1995; Pearson and Palmer, 1999; Lemarchand et al., 2002; Hönisch and Hemming, 2005; Pelejero et al., 2005) have most commonly used an isotope equilibrium constant ($^{11-10}K_B = 1.0194$ at 25 °C) for reaction (2) that was estimated, over 30 years ago, using reduced partition function calculations from spectroscopic data on molecular vibrations (Kakihana et al., 1977). This constant has been the subject of recent debate, largely based on contrasting interpretations of results

* Corresponding author.
E-mail address: klochko@umd.edu (K. Klochko).

0016-7037/$ - see front matter © 2009 Elsevier Ltd. All rights reserved.
doi:10.1016/j.gca.2009.01.002

from pH-controlled calibration studies of cultured coral, foraminifera, and inorganic calcite (Sanyal et al., 1996, 2000, 2001; Hönisch et al., 2004). Whereas control studies demonstrated a distinct relationship between the $\delta^{11}B$ of precipitated carbonates and the pH of aqueous solutions, carbonate values were systematically depleted in ^{11}B relative to the expected value for aqueous $B(OH)_4^-$, believed to be primarily boron species incorporated into the mineral lattice (Fig. 1). It has been argued (Hönisch and Hemming, 2004; Hönisch et al., 2008) that because these calibration measurements broadly mirror the "shape" of the Kakihana's curve, a constant offset at different pH may be used to empirically correct $\delta^{11}B$ values for each of the studied species. While this may be a possible solution, it does not address the underlying mechanism(s) responsible for the ^{11}B depletion. Since all imaginable processes (e.g., boric acid incorporation, metabolic seawater modification at the site of calcification, etc.) would result in ^{11}B enrichment in carbonate relative to aqueous borate, the only logical explanation is that the magnitude of $^{11-10}K_B$ was underestimated (Zeebe et al., 2003).

Subsequent studies, including new *ab-initio* calculations and semi-empirical modeling, as well as precipitation and adsorption experiments have focused on re-evaluating the magnitude of the boron isotope equilibrium constant (Palmer et al., 1987; Oi et al., 1991; Oi, 2000a, b; Sanyal et al., 2000; Sonoda et al., 2000; Oi and Yanase, 2001; Liu and Tossell, 2005; Pagani et al., 2005; Sanchez-Valle et al., 2005; Zeebe, 2005). However, until recently there have been no experimental measurements of $^{11-10}K_B$ in aqueous solutions. In our earlier publications (Byrne et al., 2006; Klochko et al., 2006), we used a spectrophotometric technique on isotopically labeled boric acid solutions to determine the magnitude of $^{11-10}K_B$, which was shown to be ca. 1.0272 ($\pm$ 0.0006, 2σ) regardless of ionic strength or boron concentration. Using the new empirical constant, the boron isotope composition of cultured carbonates in the pH controlled experiments was shown to be enriched in ^{11}B relative to the expected $\delta^{11}B$ composition of borate (see Fig. 1).

To explain the observed ^{11}B enrichments, we suggested two potential mechanisms (Klochko et al., 2006). First, $\delta^{11}B$ of biological carbonates could be affected indirectly via pH adjustment at the site of calcification. Second, boron partitioning in carbonates during mineralization might result in the non-equilibrium enrichment of ^{11}B in the experimental carbonates. Here we suggest that ^{11}B enriched boric acid may be incorporated into the carbonate lattice along with borate; hence the overall boron isotopic composition of the carbonate would be higher than expected from exclusive borate incorporation (see Section 4).

Earlier publications, however, suggested that the charged tetrahedral borate $B(OH)_4^-$ species would be preferentially attracted to mineral surfaces, substituting for the charged carbonate ion (Palmer et al., 1987; Spivack and Edmond, 1987; Hemming and Hanson, 1992). To evaluate this hypothesis, Sen et al. (1994) employed nuclear magnetic resonance (NMR) spectroscopy to quantitatively measure the relative abundance of boron species in synthetic carbonates precipitated from similar starting solutions, as well as some biogenic carbonates. These authors concluded from their NMR data that aragonite contained only tetrahedral

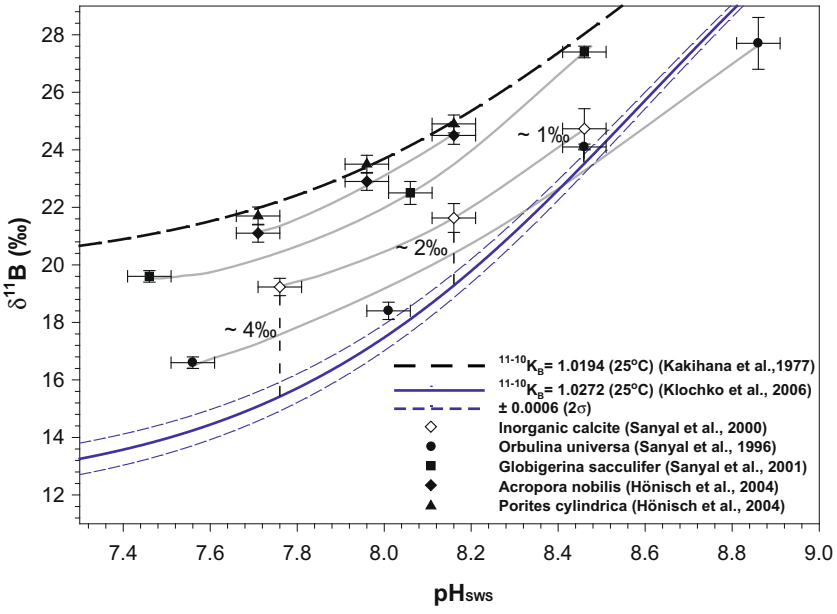

Fig. 1. $\delta^{11}B$ of $B(OH)_4^-$ in seawater based on theoretical $^{11-10}K_B = 1.0194$ (Kakihana et al., 1977) and empirical $^{11-10}K_B = 1.0272 \pm 0.0006$ (2σ) (Klochko et al., 2006); and the results of the inorganic calcite precipitation experiments (Sanyal et al., 2000), cultured *Orbulina universa* and *Globigerina sacculifer* foraminifera species (Sanyal et al., 1996, 2001) and cultured scleractinian corals *Acropora nobilis* and *Porites cylindrica* (Hönisch et al., 2004). The pH_{NBS} values from (Sanyal et al., 1996, 2000, 2001) were recalculated to fit the seawater pH scale ($pH_{SWS} = pH_{NBS} - 0.14$) (cf., Hönisch et al., 2004). The gray lines represent the polynomial best fits through the $\delta^{11}B$ data-points from precipitation experiments.

coordinated borate ion, whereas in calcite, whether natural, synthetic, or the product of a high temperature (~400 °C) phase transformation, over 90% of boron was in trigonal coordination. The inferred species dependence of boron uptake into the crystal structure of carbonates is remarkable insofar as the larger tetrahedral anion appeared to substitute into the smaller lattice sites in aragonite, whereas the smaller trigonal ion substituted into larger lattice sites in calcite. Even more interesting was the observation that the $\delta^{11}B$ of these minerals were similar (Hemming and Hanson, 1992).

To explain this phenomenon it was later suggested that there may be a structural barrier in calcite that causes a quantitative change from tetrahedral to trigonal coordination during incorporation without significant isotopic fractionation (Hemming et al., 1995, 1998). If correct, this supports the view that only borate ion, $B(OH)_4^-$, is taken up by carbonate minerals from aqueous solutions. However, the variability of $\delta^{11}B$ in calcite samples from later experiments (Sanyal et al., 1996, 2000, 2001; Hönisch et al., 2004) and the observation that aragonite is consistently enriched in ^{11}B relative to calcite over a range of pH are difficult to reconcile with the NMR results (Sen et al., 1994).

In this study we re-investigate borate speciation in biogenic and hydrothermal carbonates using solid state ^{11}B magic angle spinning (MAS) NMR spectroscopy. Our new results contrast strongly with those of Sen et al. (1994) as we observe both trigonal and tetrahedral coordinated boron in almost equal abundances in the biogenic calcite and aragonite samples. Moreover, we observe no strict dependency of boron coordination on the carbonate crystal structure.

2. METHODS

2.1. Samples

Two scleractinian coral samples, *Diploria strigosa* and *Porites* sp., originally collected for a detailed study of carbon and nitrogen isotopes (Jabo, 2001), were obtained for the NMR experiments. The *D. strigosa* sample was collected from Three Hills Shoal (depth of 3–4.5 m) in Bermuda, and the *Porites* sp. sample was collected from Pickles Reef (depth 4.5–6 m) in Florida. Organic components (i.e., coral animal, algal symbionts, and endolithic algae) within these corals were removed by physical separation with a Waterpik® followed by an overnight treatment with 1 M NaOH. Samples were then ultra-sonicated in Milli-Q water (Jabo, 2001). Between 100 and 200 mg of each prepared coral was isolated with a drill and fragments crushed to a fine powder in an agate mortar with pestle for our ^{11}B NMR analysis. X-ray diffraction (XRD) analyses indicated that aragonite was the only mineral present in both samples.

A foraminifera sample of *Assilina ammonoides* was obtained from the Reef Indicators Lab at the College of Marine Sciences, University of South Florida, St. Petersburg. This sample was collected from Tutum Bay off the coast of Papua New Guinea. The sample was stored and shipped in ethanol, which was removed by repeated sonication with Milli-Q water. After drying, the sample was crushed to a fine powder in an agate mortar with pestle for ^{11}B NMR analysis. XRD analysis identified only calcite in this sample.

For comparative purposes, we analyzed a well characterized carbonate sample (#3651-0908) (Ludwig et al., 2006) from the Lost City Hydrothermal Field carbonate chimneys (Kelley et al., 2001, 2005). The Lost City carbonate chimneys are remarkable structures that form rapidly during mixing of Ca^{2+} bearing alkaline fluids with ocean water. Based on the chemistry of fluids emitted from active structures in the vicinity, the source water for the sample #3651-0908 had pH >10 at temperatures near 60 °C (Ludwig et al., 2006). The sample was collected at a depth of 844 m and currently contains a mixture of calcite and high magnesium calcite, but no aragonite.

2.2. X-ray diffraction

X-ray diffraction analyses of the samples were performed with a Rigaku RAXIS/RAPID diffractometer with an Ultrax-18, 18 kW rotating anode X-ray generator and a hemi-cylindrical image-plate detector at the Carnegie Institution for Science. Twenty minute exposures were taken using monochromatic, Mo Kα radiation. Samples were oscillated over a 40° range to average grain orientations. Crystal structure of the biogenic samples was established via their characteristic diffraction patterns. In either case, the calcite and aragonite samples are determined to be 99% mineralogically pure.

2.3. ^{11}B MAS NMR spectroscopy

^{11}B MAS NMR analyses were performed at the W.M. Keck solid state NMR facility at the Geophysical Laboratory, Carnegie Institution for Science. The instrument used in this study is a three channel Varian-Chemagnetics Infinity solid state NMR spectrometer. The static field strength of the magnet is ~7.05 T, a lower field than the system used by Sen et al. (9.4 T). As discussed below, peak positions, width and shape depend on the field dependence of the quadrupolar interaction. The Larmor frequency of ^{11}B in this static magnetic field is 96.27 MHz. For the current experiments, 100–200 mg of powdered samples were placed in 5 mm diameter zirconia rotor cells. The sample was spun at a magic angle of 54.7° at a frequency ($\omega_r/2\pi$) of 12 kHz. All experiments employed an excitation RF pulse that corresponds to a 10° tip angle with RF power ($\omega_1/2\pi$) of 56 kHz; high power RF decoupling ($\omega_1/2\pi = 65$ kHz) was applied during signal acquisition to mitigate the effects of ^1H–^{11}B dipolar coupling. The recycle delay between acquisitions was 0.5 s and a total of 300,000 acquisitions were sufficient to resolve the characteristic borate spectral features. All spectra are referenced to the resonant frequency of boron trifluoride diethyl etherate defined as equal to 0 ppm.

3. RESULTS

Solid state ^{11}B NMR spectroscopy is particularly well suited to provide fundamental information about the speciation of boron in carbonates. Acknowledging that the pri-

mary audience for this study are paleo-oceanographers, a brief discussion about ^{11}B NMR is warranted. The ^{11}B nucleus is a spin 3/2 particle that has both a magnetic dipole and electric quadrupole moment. The presence of an electric quadrupole moment means that the nucleus will interact strongly with the local electric field surrounding the nucleus. This interaction has a significant effect on the observed spectrum. The strength of local electric field gradient (EFG) is described by a second rank tensor with principal axis elements V_{ii} ($i = x$, y, and z) (Cohen and Reif, 1957). The symmetry of the EFG manifests predictable and large effects in the spectral line shape of ^{11}B species in the solid state and is quantified by the asymmetry parameter, η [$\eta = (V_{xx} - V_{yy})/V_{zz}$)]. In the case of perfect radial symmetry of the EFG around the quadrupolar nucleus ($V_{xx} = V_{yy}$) $\eta = 0$, and in the case maximum deviation away from cylindrical symmetry, $\eta = 1$. In the case where the EFG is perfectly spherically symmetric around the nucleus, $V_{xx} = V_{yy} = V_{zz} = 0$ and the quadrupolar interaction is nonexistent (i.e., the spins respond to radiofrequency pulses through their magnetic dipole interaction only). Static NMR experiments show that the shape of the resultant powder patterns is strongly affected by the value of η. In the case of borate salts and boric acid, the BO_3 species have a nearly perfect trigonal planar distribution of oxygen atoms surrounding the ^{11}B nucleus, consequently η is observed to be nearly equal to zero (note that if BO_3 groups are covalently bonded to other cations through bridging oxygens, then a significant distortion of the EFG away from trigonal symmetry will occur). The BO_4 species have a tetrahedral oxygen arrangement that approaches nearly perfect cubic symmetry; thus, a minimal quadrupolar interaction for these borate species is expected and observed.

In the present experiments, powder samples were spun rapidly at the magic angle, 54.7°, during signal acquisition. Magic angle sample spinning (MAS) is performed in order to average out chemical shielding anisotropy, some of the quadrupolar broadening, as well as to reduce broadening associated with proton dipolar coupling (thus enhancing the effectiveness of RF decoupling). In the case of the quadrupolar interaction, rapid MAS at 54.7 °C cannot completely average out the fourth rank tensorial terms of the quadrupolar Hamiltonian (Ganapathy et al., 1982), although it does afford significant line narrowing compared to static NMR improving the signal to noise. This means that even with fast MAS one can readily distinguish between boron sites with dramatically different EFG symmetries (e.g., BO_3 and BO_4).

In Fig. 2, the ^{11}B MAS NMR spectrum (with ^{1}H decoupling) is presented for a pure $B(OH)_3$ standard, revealing the characteristic two-peak MAS quadrupolar powder pattern for a single boron site with a radially symmetric EFG. This single site is adequately fit with η set equal to 0, a quadrupolar coupling parameter, C_q, set to 2.5 MHz, an isotropic shift, δ_{iso} set to 19 ppm, and a modest amount of line broadening, 140 Hz (Massiot et al., 2002). In Fig. 3a–c, ^{11}B MAS NMR spectra are presented for three natural biological specimens of carbonate, including calcite (foraminifera *A. ammonoides*, Fig. 3a) and aragonite (corals *D. strigosa*, Fig. 3b, and *Porites* sp., Fig. 3c). In each case,

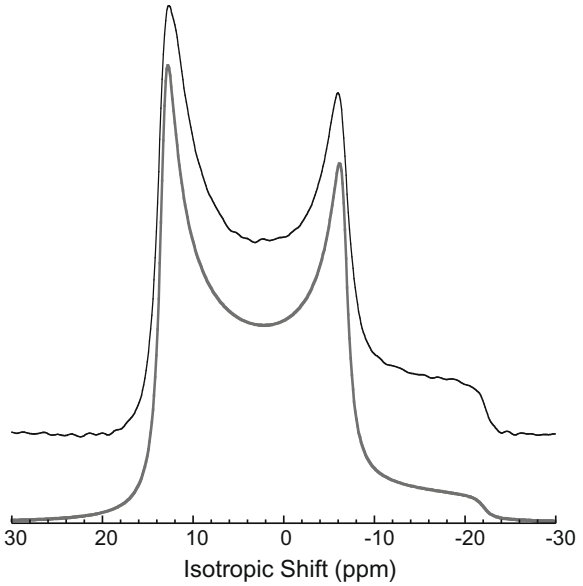

Fig. 2. ^{11}B MAS NMR spectrum of boric acid standard, $B(OH)_3$. A single boron site is observed that exhibits a classic MAS quadrupolar power pattern resulting from the inability of spinning at 54.7° to average out fourth rank tensorial terms of the quadrupolar Hamiltonian. A simulation (fit) of this spectrum is presented by the bold line spectrum where the following parameters were used, $\eta = 0.0$, $C_q = 2.470$ MHz, and $\delta_{iso} = 19$ ppm. These parameters are consistent with a highly symmetrical trigonal BO_3 site. Boric acid $B(OH)_3$ (ACS reagent, $\geqslant$99.5% pure) obtained from Sigma–Aldrich was used as a standard in this study.

satisfactory fits of the spectra are achieved with two boron species, BO_3 fit with η fixed at 0 and adjustment of the line broadening and a BO_4 species fit with a single Lorentzian line, assuming that $C_q = 0$. Slightly better fits (i.e., achieving lower residuals) are achievable if a mixed Lorentzian/Gaussian broadening function is used. For the current purposes, however, the original fits are sufficient to show that each of these biological carbonates contain mixed borate species with a slight predominance of BO_4 over BO_3. The various NMR parameters as well as species abundances are presented in Table 1.

To test whether the solution pH has any effect on the borate speciation in the carbonate structure, we analyzed the Lost City carbonate sample which precipitated from solutions of pH >10 (Ludwig et al., 2006). The ^{11}B MAS NMR spectrum for this sample is presented in Fig. 4 where only BO_4 was detected. For the present discussion, the presence of essentially pure BO_4 in this hydrothermal calcite is important insofar as it suggests that there exists no structural barrier to the incorporation of the larger tetrahedral borate species in calcite, as was previously suggested (Sen et al., 1994; Hemming et al., 1995, 1998). We acknowledge that a rapid precipitation rate, as expected for this hydrothermal chimney sample, may favor the incorporation of the dominant species in solution, even if it is less stable in the crystalline structure.

In the present experiments, high power RF ^{1}H decoupling was applied during the signal acquisition phase based

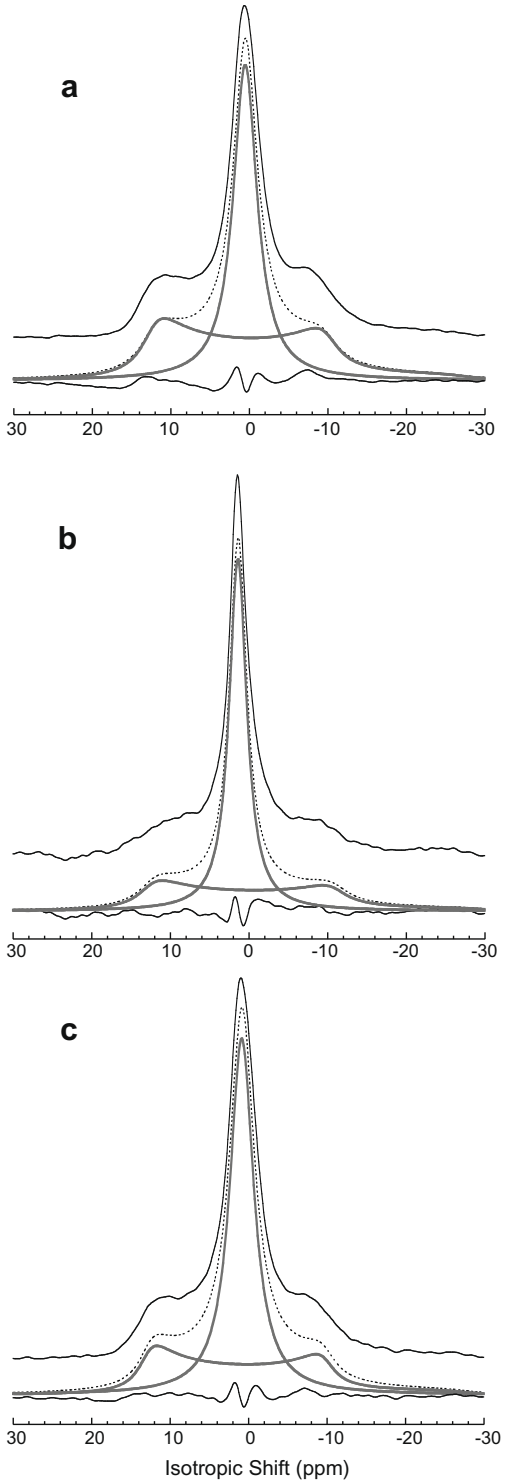

Fig. 3. ^{11}B MAS NMR of three biogenic carbonates revealing that borate is present in both trigonal and tetrahedral coordination: (a) calcite from the foraminifera (*Assilina ammonoides*) with BO_3 (~46%) and BO_4 (~54%); (b) aragonite from the coral (*Diploria strigosa*) with BO_3 (~36%) and BO_4 (~64%); and (c) aragonite from the coral (*Porites* sp.) with BO_3 (~36%) and BO_4 (~64%). The total fit is shown as a dotted line; the individual sites are shown in bold black. The difference between the spectrum and the fit is in black. The acquired spectrum is in black and offset vertically from the total fit.

on the assumption that boron is incorporated into a growing carbonate as $B(OH)_3$ or $B(OH)_4^-$ (i.e., analogous to recent observations that HCO_3^- groups can be incorporated into growing carbonate as detected in a recent solid state NMR study) (Feng et al., 2006). In the case of spin 1/2 nuclei, ^1H decoupling provides greater spectral resolution by reducing the magnitude of this homogeneous source of line broadening. In the case of proton coupling to quadrupolar nuclei (e.g., ^{11}B), however, there is an additional issue; in addition to broadening there is also distortion of the rotational powder pattern due an orientational dependence on ^1H–^{11}B coupling interaction that is moderated by the fast MAS. This combination of line broadening and spectral distortion is clearly manifested in Fig. 5 where $B(OH)_3$ MAS NMR without ^1H decoupling is compared with the same experiment with ^1H decoupling.

Similarly, the same orientational distortion of the "BO_3" MAS powder pattern is clearly observed when comparing the borate spectra of the carbonates (e.g., *Porites* sp.) with and without ^1H decoupling, revealing the presence of neighboring H^+ atoms (Fig. 6). There is, however, a spectral distortion of a different sort that provides additional information. Without decoupling, the "BO_3" intensity appears enhanced relative to the "BO_4" intensity when normalized to the spectrum obtained with decoupling. The most likely explanation for this distortion is that the "BO_4" groups are associated with more hydrogen atoms than the BO_3 groups, and hence experience a more intense dipolar perturbation leading to greater line broadening. These results suggest that additional experiments might be performed to gain better insights on the true stoichiometry of the protonated borate structures in these carbonates. It should also be noted that even with ^1H RF decoupling, the BO_3 resonance features in the biogenic carbonates are broader than that of the $B(OH)_3$ standard (Table 1). This residual broadening may be due to inhomogeneous effects (e.g., slight positional disorder in the anionic site) or may reflect the presence of paramagnetic species in the natural carbonates (e.g., Mn^{2+}).

The new measurements reveal the presence of both BO_3 and BO_4 groups in both aragonite and calcite. In contrast, Sen et al. (1994) concluded, from their spectra analysis, that BO_3 groups are predominantly incorporated into calcite. Inspection of their data confirms the presence of a small amount of BO_4 groups in their calcite sample. It is noteworthy, however, that the calcite ^{11}B NMR spectrum acquired by Sen et al. (1994) differs significantly from the spectral signature of BO_3 groups that we observe in this study. Notably, Sen et al. (1994) report a η of up to 0.67 and a C_q on the order of 3.0 MHz. These values are vastly different from what is expected and observed for the trigonal $B(OH)_3$ and indicate that the symmetry of the EFG surrounding ^{11}B in their calcite sample is not radially symmetric. Sen et al. (1994) acquired their data at a static magnetic field of 9.4 T, whereas the present experiments were acquired at ~7.05 T. In order to compare the calcite spectrum of Sen et al. (1994) with the one we obtained of the foraminiferal calcite (Fig. 3a), we simulated the Sen et al. (1994) spectrum as it would appear at ~7.05 T. This comparison is presented in Fig. 7 revealing that the boron site detected

Table 1
^{11}B MAS NMR parameters, where δ_{iso}, isotropic chemical shift, expressed in parts per million; C_q, nuclear quadrupolar coupling constant, expressed in MHz; LB, line broadening, expressed in Hz; η, EFG asymmetry parameter.

Sample	Mineralogy	BO_3				BO_4			
		δ_{iso}	C_q	LB	η	δ_{iso}	C_q	LB	η
Coral *Diploria strigosa*	100% Aragonite	16.8	2.5	469.9	0	2.54	0	—	—
Coral *Porites* sp.	100% Aragonite	18.3	2.5	361.5	0	2.0	0	—	—
Foram *Assilina ammonoides*	100% Calcite	19.3	2.6	455.9	0	1.67	0	—	—
Lost City carbonate #3651-0908	Calcite/Mg-calcite	—	—	—	—	2.85	0	—	
Boric acid standard	—	19.5	2.5	114.7	0	—	—	—	—

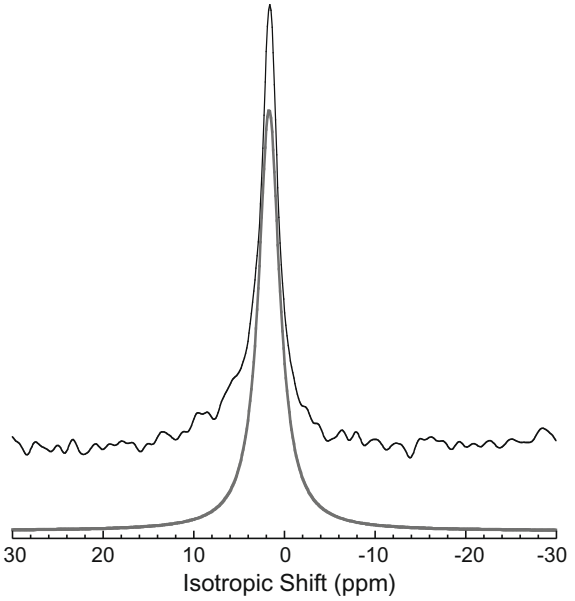

Fig. 4. ^{11}B MAS NMR of a deep sea serpentinite carbonate from the Lost City Hydrothermal complex and precipitated at high pH. The entire spectrum is adequately fit with single Lorentzian line with similar isotropic shift to that of other BO_4 groups in calcite and aragonite.

by Sen et al. (1994) is completely different from the present observations for the foraminiferal calcite.

Clearly, we are observing different borate structures. A clue to what Sen et al. (1994) likely detected may be found in an extensive theoretical analysis of boric acid adsorption on humic acids (Tossell, 2006). One of the species for which Tossell (2006) calculated NMR and NQR properties was the corner-sharing borate carbonate complex, $B(OH)_2CO_3^-$. His calculations yield a theoretical value for η of 0.54 and a C_q of 3.15 MHz. Not surprisingly, covalent bonding of the $B(OH)_3$ group to the CO_3^{-2} anion significantly distorts the trigonal arrangement of oxygen atoms and the EFG far from cylindrical symmetry. In Fig. 8, we present a simulation of the ^{11}B MAS spectrum for $B(OH)_2CO_3^-$ along with the boron site observed in calcite by Sen et al. (1994). The spectra of these two sites are very similar supporting the previous suggestion by Tossell (2006) that Sen et al. (1994) had actually detected $B(OH)_2CO_3^-$ impurities incorporated in calcite. Intriguingly, Sen et al.'s (1994) study likely identified boron incorporation as $B(OH)_2CO_3^-$ in their synthetic calcite, a species not observed in carbonate samples analyzed in this study.

4. DISCUSSION

The principle goal of using boron isotopes in carbonates is to accurately predict the pH of ambient solutions. The equation relating solution pH, boron isotopic composition of boron species incorporated in the carbonate mineral ($\delta^{11}B_{BSp}$) and of seawater ($\delta^{11}B_{sw} = 39.5‰$) is expressed as:

$$\mathrm{pH} = \mathrm{p}K_B - \log\left(\frac{\delta^{11}B_{sw} - \delta^{11}B_{BSp}}{\delta^{11}B_{sw} - {}^{11-10}K_B\delta^{11}B_{BSp} - 1000 \times ({}^{11-10}K_B - 1)}\right), \quad (3)$$

which depends on three key variables: (1) the boron isotope exchange constant between borate ion and boric acid in solution—$^{11-10}K_B$, (2) the boron species partitioning into carbonate, which ultimately determines $\delta^{11}B_{BSp}$, and (3) the boric acid stoichiometric dissociation constant—pK^*_B. In our earlier publication (Klochko et al., 2006) we address the first variable; in this study we address the second, in particular the deviations in $\delta^{11}B$ of biogenic and inorganic precipitates from empirical calibration studies (Sanyal et al., 1996, 2000, 2001; Hönisch et al., 2004).

Three key observations of the culture data require explanation. First, with the exception of a single data point, all carbonates precipitated under controlled pH conditions were enriched in ^{11}B relative to seawater borate, as characterized by the larger fractionation constant (Klochko et al., 2006) (Fig. 1). Second, the ^{11}B enrichments are more pronounced at lower pH; and third, $\delta^{11}B$ values between calcifying species are variable. Since metabolic and inorganic processes may differentially affect boron isotope distributions in carbonates, we address biogenic and inorganic precipitates separately.

4.1. Biologically driven effects

Boron isotope redistribution during biosynthesis of carbonate is likely, given that biomineralizing organisms may actively modify seawater composition (carbonate ion concentration and saturation state) at the site of calcification (Erez, 2003; Weiner and Dove, 2003). Saturation is usually maintained by seawater isolation and active modification, and is usually accompanied by elevation of both pH and alkalinity in the calcifying fluid (Weiner and Dove, 2003).

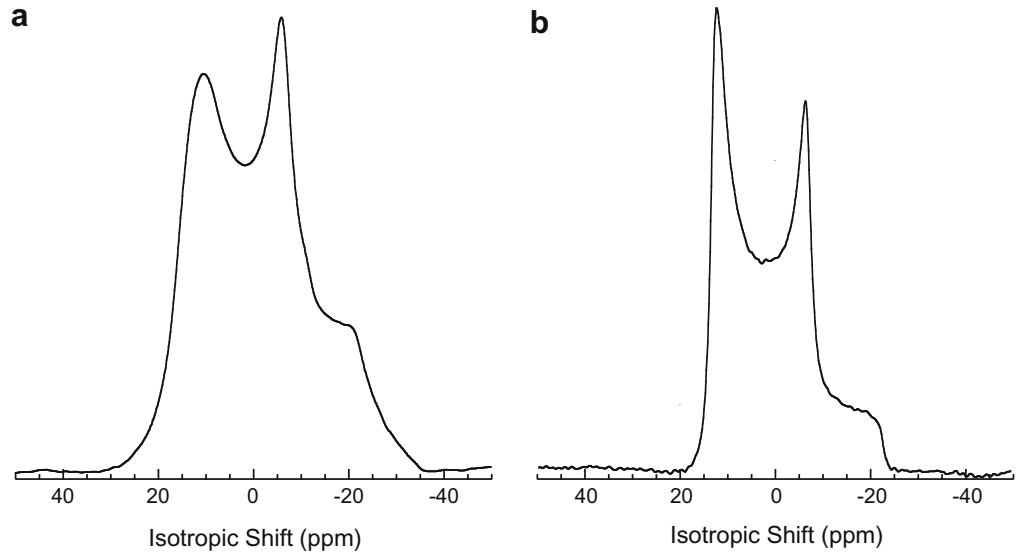

Fig. 5. A comparison of ^{11}B MAS NMR spectra of boric acid, $B(OH)_3$: (a) acquired without high power RF ^1H decoupling; (b) acquired with high power RF ^1H decoupling ($\omega_1/2\pi = 75$ kHz). Note that, without decoupling, one observes both line broadening and spectral distortion.

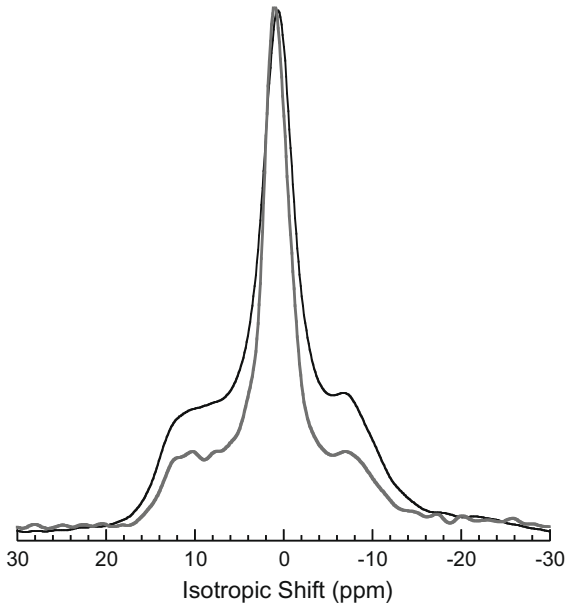

Fig. 6. An overlay of ^{11}B MAS NMR spectra of the coral *Porites* sp., in bold black: acquisition with high power RF ^1H decoupling. In black: acquisition without RF decoupling. The apparent increase in BO_3 intensity in the absence of high power RF ^1H decoupling suggests greater H coordination in the case of the BO_4 groups.

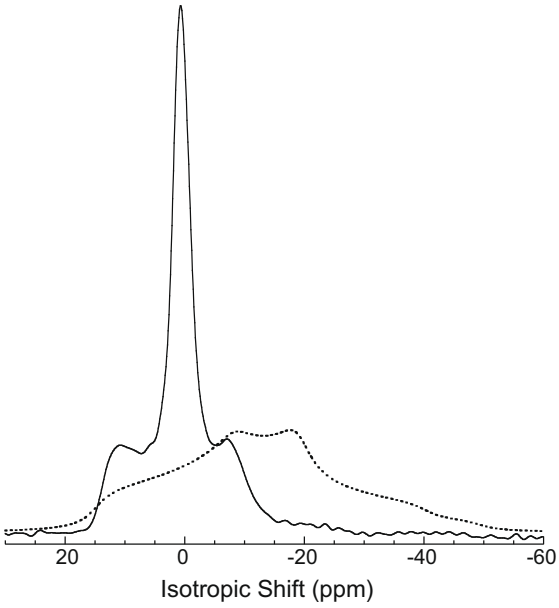

Fig. 7. A comparison of the ^{11}B MAS NMR spectrum of foraminifera calcite (this study, where both BO_3 and BO_4 are observed, solid line) with a simulation (for an external magnetic field of 7 T) of the boron site previously observed and reported in synthetic calcite (at an external magnetic field of 9.4 T) (Sen et al., 1994, dotted line). The enormous differences in peak shape results from large differences in the symmetry of the electric field gradient (η) as well as in the magnitude of the quadrupolar coupling parameter (C_q).

Current models suggest that Ca^{2+}, CO_2, and other seawater constituents enter the site of calcification through vacuolization in foraminifera (Erez, 2003), whereas in corals, endergonic enzymatic reactions that exchange protons for Ca^{2+} result in higher pH at the site of calcification (Allemand et al., 1998; Cohen and McConnaughey, 2003). Micro-sensor studies indicate that the pH of the calcifying fluid in the foraminifera *G. sacculifer* rises to as high as 8.6 in daylight (Jorgensen et al., 1985). Similarly, pH in the symbiotic coral *Galaxea* rises from 8.2 to 8.5 at the polyp surface and further to 9.3 in the calcifying fluid (Al-Horani et al., 2003). Unfortunately, it is not known whether there is a preference

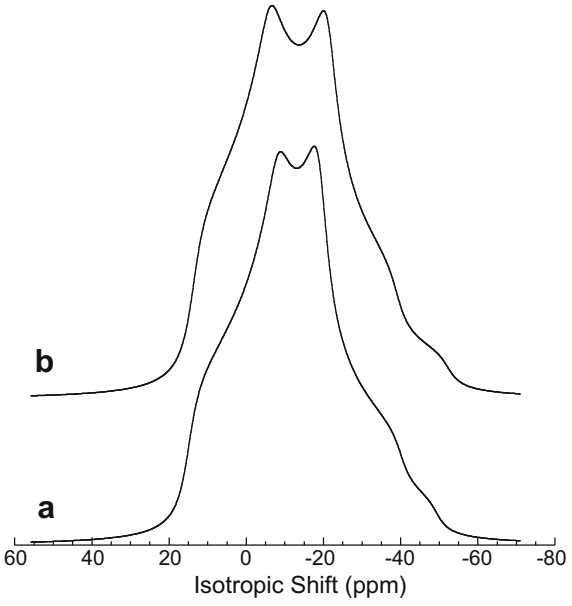

Fig. 8. A comparison of simulations of: (a) the boron site previously observed and reported in synthetic calcite (at an external magnetic field of 9.4 T) (adopted from Sen et al., 1994); (b) the MAS quadrupolar powder pattern predicted for corner linked mixed borate-carbonate species $B(OH)_2CO_3^-$ (adopted from Tossell, 2006).

for neutral $B(OH)_3^0$ or charged $B(OH)_4^-$ during boron uptake into the calcifying site or if there is simply a bulk uptake of seawater boron species. In either case, if the pH of the calcifying fluid is higher than that of seawater, re-equilibration between $B(OH)_3^0/B(OH)_4^-$ must occur upon their introduction in these higher pH conditions. Hence, reaction (1) shifts to the right to satisfy chemical equilibrium. As a result, some borate in the calcifying fluid could be formed from the dissociation of boric acid and thus bear its ^{11}B enriched isotopic signature. This effect would be more pronounced at lower ambient seawater pH because the pH adjustment to reach supersaturation would be larger, hence requiring the conversion of more boric acid to borate ion (Fig. 1).

This proposed mechanism, however, cannot explain significant differences in δ^{11}B data between various cultured organisms (the so-called "species effect") (Sanyal et al., 1996, 2001; Hönisch et al., 2004). In this analysis, we accept the literature data at face value, although the accuracy of the NTIMS (negative ion thermal ionization mass spectrometry) approach has been recently questioned (Foster, 2008) given the differences in ionization characteristics between foraminiferal carbonate (containing trace organic material) and the normalizing standard solution (boric acid + boron free seawater). Although relative differences in δ^{11}B may be reconstructed using NTIMS with some degree of confidence, the 4‰ range reported from different laboratories for the same species of planktonic foraminifera highlights the difficulty of generating accurate δ^{11}B data using this approach (see Foster, 2008).

In addition to inter-species δ^{11}B variations and enrichments, ^{11}B enrichments are observed in inorganic calcite relative to aqueous borate, where biological effects would not be present (Fig. 1). This observation suggests that inorganic processes, likely associated with the complexation of boron species during carbonate precipitation, may also result in boron isotope redistribution.

4.2. Inorganic effects

Inorganic effects may manifest themselves during the complex mechanism of boron incorporation from solution to its position in the carbonate structure (Fig. 9). For example at the dissociation/isotope exchange stage (Stage I), pH-driven distribution of the $B(OH)_4^-$ and $B(OH)_3$ species as well as the isotope exchange between these species occurs in solution. This stage, which defines the isotopic composition of both species in solution at a set pH, is fairly well characterized. The subsequent steps in the boron incorporation pathway into the carbonate are less well defined. It has been proposed that $B(OH)_4^-$ species preferentially adsorb on to the carbonate surface; subsequent coordination change from BO_4 to BO_3 could then occur during incorporation into the growing carbonate, hence preserving the solution pH derived ^{11}B isotopic abundance (Sen et al., 1994; Hemming et al., 1998).

Boron incorporated into carbonate minerals precipitated inorganically under pH-controlled conditions (Sanyal et al., 2000) appears to carry an isotopic signature close to the aqueous borate, supporting the idea that borate is preferentially incorporated into the carbonate. Nevertheless, at lower pH there appears to be a progressive enrichment in ^{11}B relative to aqueous borate. For example, the positive offset between δ^{11}B of inorganic calcite (Sanyal et al., 2000) and aqueous borate (Klochko et al., 2006) is ~4‰, 2‰, and 1‰ at pH 7.6, 8.2, and 8.5, respectively (Fig. 1). As boric acid ($B(OH)_3$) becomes the predominant boron species in seawater at pH <8.587 (Dickson, 1990), and its relative concentration increases with decreasing pH, it is reasonable to assume that its contribution to the incorporation of boron into the carbonate should also increase leading to larger deviations of the δ^{11}B in carbonates from the borate curve.

Based on this ^{11}B MAS NMR study of three modern biogenic carbonates, we observe a substantial presence of BO_3 (36–46%) in both aragonite and calcite minerals. If all the boric acid were to come directly from the seawater, then the isotopic composition of studied carbonates should be close to that of seawater (~39.5‰), which is inconsistent with the δ^{11}B data available for the natural and synthesized carbonates. This suggests that changes in coordination of the boron species indeed occur during carbonate precipitation (Sen et al., 1994; Hemming et al., 1998).

It is interesting to consider whether such a coordination change might occur through an intermediate phase, such as hypothesized by Tossell (2006). In that study, it was proposed that boron incorporation does not occur by simple adsorption of the borate species to the carbonate surface. Instead, chemical reactions between HCO_3^- and either $B(OH)_3$ or $B(OH)_4^-$ take place on carbonate surfaces during the early growth phase (Stage II) (Tossell, 2006). During this "chemosorption" stage, $B(OH)_2CO_3^-$ isomers of either

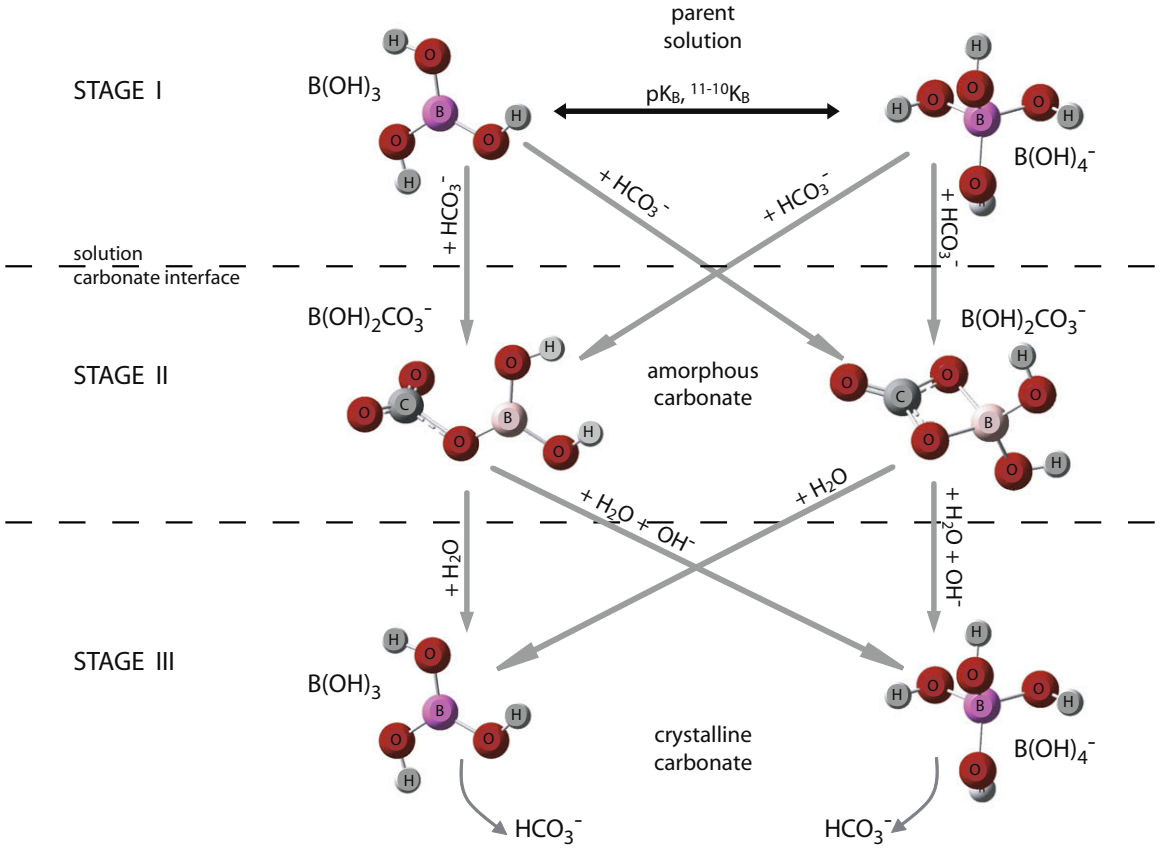

Fig. 9. Proposed stage-model of boron incorporation into a carbonate. Schematic representations of molecular structures are adopted from Tossell (2006). Complete reactions for the processes graphically presented in the model are the following: (1) $B(OH)_3 + H_2O \Longleftrightarrow B(OH)_4^- + H^+$, (2) $^{10}B(OH)_3 + {}^{11}B(OH)_4^- \Longleftrightarrow {}^{11}B(OH)_3 + {}^{10}B(OH)_4^-$, (3) $B(OH)_3 + HCO_3^- \Longleftrightarrow B(OH)_2CO_3^- + H_2O$,(4) $B(OH)_4^- + HCO_3^- \Longleftrightarrow B(OH)_2CO_3^- + H_2O + OH^-$, (5) $B(OH)_2CO_3^- + H_2O \Longleftrightarrow B(OH)_3 + HCO_3^-$, (6) $B(OH)_2CO_3^- + H_2O + OH^- \Longleftrightarrow B(OH)_4^- + HCO_3^-$.

trigonal (oxygen-corner-sharing) or tetrahedral (oxygen four-ring) coordination form on the surface (Fig. 9).

As the free energy of formation of these two isomers are very similar, the likelihood of either reaction occurring will essentially be equal. During Stage III, the $B(OH)_2CO_3^-$ isomers, once in the carbonate structure, may break down to the simpler forms and coordination of BO_3 or BO_4, which could explain why we detect only simple BO_3 and BO_4 groups in natural carbonates by NMR.

Although, $B(OH)_2CO_3^-$ isomer formation was investigated (McElligott and Byrne, 1998; Tossell, 2006), the existence of these isomers has never been demonstrated. Nevertheless, it is interesting to note that the ^{11}B MAS NMR spectra of the synthetic calcite analyzed by Sen et al. (1994) is consistent with the simulated spectra of the oxygen-corner-sharing $B(OH)_2CO_3^-$ species (Tossell, 2006) (Fig. 8). The rate at which Sen et al.'s synthetic calcite was precipitated may have been fast enough that the $B(OH)_2CO_3^-$ anion was incorporated directly whereas, in the case of biogenic calcite, this species is hydrolyzed prior to precipitation (Stage III). While speculative, the study of Tossell (2006) suggests that any of the reactions during Stages II and III of boron incorporation in carbonate minerals could result in boron isotope redistribution and are most likely to determine the ultimate bulk boron isotopic composition observed in carbonates.

5. CONCLUSIONS

Based on our ^{11}B MAS NMR study of three modern biogenic carbonates: two coral aragonites and one foraminiferal calcite, we find no evidence for a strong dependency of boron coordination on crystal structure. Rather, we observe close similarity between these carbonate samples in terms of the relative proportion of boron species, with BO_3 and BO_4 groups representing roughly 36–46% and 54–64%, respectively. Boric acid incorporation may contribute to the ^{11}B enrichment observed in inorganic and biogenic precipitated carbonates, even more so at lower pH, but it is unlikely that all the BO_3 coordinated species detected in calcite and aragonite of our NMR study could come directly from seawater. The observed BO_3/BO_4 inventory in these minerals is likely the product of some reconstructive surface processes occurring during mineralization, which might involve boron isotope fractionation.

Together, these NMR results and our earlier experimental measurements of $^{11-10}K_B$ in aqueous solutions (Byrne et al., 2006; Klochko et al., 2006) indicate that the controls

on the boron isotope composition in biological marine carbonates are more complex that previously suggested. We believe that additional testing of the proxy is warranted prior to its further application in paleoceanographic research. In this regard we are presently conducting pH controlled inorganic precipitation experiments (e.g., Kim et al., 2006) to quantitatively evaluate boron speciation and isotope distribution in carbonates, which should provide more rigorous constraints on the system.

ACKNOWLEDGMENTS

This manuscript benefited greatly from the editorial remarks of the Associate Editor (Alfonso Mucci), Damien Lemarchand, two anonymous reviewers, and our colleague George Helz. We thank Chris Langdon and Gavin Foster, who provided important insights. We also thank Deborah S. Kelley (University of Washington, Seattle) and Gretchen Früh-Green (ETH-Zürich, Switzerland) for providing us with the Lost City carbonate sample; Brian McCloskey and Pamela Hallock-Muller (University of South Florida, St. Petersburg) for providing the foraminifera sample. K.K. thanks Phil Candela for encouraging discussions. This work was supported by NSF research grant NSF EAR 05-39109 to J.A. Tossell. NMR spectroscopy analyses were performed at the W.M. Keck solid state NMR facility at the Geophysical Laboratory that was supported by generous grants from the W.M. Keck Foundation, the NSF, and the Carnegie Institution for Science. A.J.K. acknowledges the Deutsche Forschungsgemeinschaft (Mu 40/91-1) for sabbatical funding.

REFERENCES

Al-Horani F. A., Al-Moghrabi S. M. and de Beer D. (2003) The mechanism of calcification and its relation to photosynthesis and respiration in the scleractinian coral *Galaxea fascicularis*. *Mar. Biol.* **142**, 419–426.

Allemand D., Tambutte E., Girard J.-P. and Jaubert J. (1998) Organic matrix synthesis in the scleractinian coral stylophora pistillata: role in biomineralization and potential target of the organotin tributyltin. *J. Exp. Biol.* **201**, 2001–2009.

Byrne R. H., Yao W., Klochko K., Tossell J. A. and Kaufman A. J. (2006) Experimental evaluation of the isotopic exchange equilibrium $^{10}B(OH)_3 + {}^{11}B(OH)_4^- = {}^{11}B(OH)_3 + {}^{10}B(OH)_4^-$ in aqueous solution. *Deep-Sea Res. I* **53**, 684–688.

Cohen A. and McConnaughey T. A. (2003) Geochemical perspectives on coral mineralization. *Rev. Mineral. Geochem.* **54**, 151–187.

Cohen M. H. and Reif F. (1957) Quadrupole effects in nuclear magnetic resonance studies of solids. *Solid State Phys.* **5**, 322–348.

Dickson A. G. (1990) Thermodynamics of the dissociation of boric acid in synthetic seawater from 273.15 to 318.15 K. *Deep-Sea Res.* **37**, 755–766.

Erez J. (2003) The source of ions for biomineralization in foraminifera and their implications for paleoceanographic proxies. *Rev. Mineral. Geochem.* **54**, 115–149.

Feng J., Lee Y. J., Reeder R. J. and Phillips B. L. (2006) Observation of bicarbonate in calcite by NMR spectroscopy. *Am. Mineral.* **91**, 957–960.

Foster G. L. (2008) Seawater pH, pCO_2 and $[CO_3^{2-}]$ variations in the Caribbean Sea over the last 130 kyr: a boron isotope and B/Ca study of planktic foraminifera. *Earth Planet. Sci. Lett.* **271**, 254–266.

Ganapathy S., Schramm S. and Oldfield E. (1982) Variable-angle sample-spinning high resolution NMR of solids. *J. Chem. Phys.* **77**, 4360–4365.

Gillardet J. and Allègre C. J. (1995) Boron isotopic compositions of corals: seawater or diagenesis record? *Earth Planet. Sci. Lett.* **136**, 665–676.

Hemming N. G. and Hanson G. N. (1992) Boron isotopic composition and concentration in modern marine carbonates. *Geochim. Cosmochim. Acta* **56**, 537–543.

Hemming N. G., Reeder R. J. and Hanson G. N. (1995) Mineral–fluid partitioning and isotopic fractionation of boron in synthetic calcium carbonate. *Geochim. Cosmochim. Acta* **59**, 371–379.

Hemming N. G., Reeder R. J. and Hart S. R. (1998) Growth-step-selective incorporation of boron on calcite surface. *Geochim. Cosmochim. Acta* **62**, 2915–2922.

Hönisch B., Bickert T. and Hemming N. G. (2008) Modern and Pleistocene boron isotope composition of the benthic foraminifer *Cibicidoides wuellerstorfi*. *Earth Planet. Sci. Lett.* **272**, 309–318.

Hönisch B. and Hemming N. G. (2004) Ground-truthing the boron isotope-paleo-pH proxy in planktonic foraminifera shells: partial dissolution and shell size effects. *Paleoceanography* **19**. doi:10.1029/2004PA001026.

Hönisch B. and Hemming N. G. (2005) Surface ocean pH response to variations in pCO_2 through two full glacial cycles. *Earth Planet. Sci. Lett.* **236**, 305–314.

Hönisch B., Hemming N. G., Grottoli A. G., Amat A., Hanson G. N. and Bijma J. (2004) Assessing scleractinian corals as recorders for paleo-pH: empirical calibration and vital effects. *Geochim. Cosmochim. Acta* **68**, 3675–3685.

Jabo A. (2001) The fractionation of carbon and nitrogen isotopes in scleractinian corals. M.Sc. thesis, University of Maryland.

Jorgensen B. B., Erez J., Revsbech N. P. and Cohen Y. (1985) Symbiotic photosynthesis in a planktonic foraminifera *Globigerinoides sacculifer* (Brady), studied with microelectrodes. *Limnol. Oceanogr.* **30**(6), 1253–1267.

Kakihana H., Kotaka M., Satoh S., Nomura M. and Okamoto M. (1977) Fundamental studies on the ion-exchange separation of boron isotopes. *Bull. Chem. Soc. Jpn.* **50**, 158–163.

Kelley D. S., Karson J. A., Blackman D. K., Früh-Green G. L., Butterfield D. A., Lilley M. D., Olson E. J., Schrenk M. O., Roe K. K., Lebon G. T. and Rivizzigno P. (2001) An off-axis hydrothermal vent field near the Mid-Atlantic Ridge at 30°N. *Nature* **412**, 145–149.

Kelley D. S., Karson J. A., Früh-Green G. L., Yoerger D., Shank T. M., Butterfield D. A., Hayes J. M., Schrenk M. O., Olson E. G., Proskurowski G., Jakuba M., Bradley A., Larson B., Ludwig K., Glickson D., Buckman K., Bradley A. S., Brazelton W. J., Roe K., Elend M. J., Delacour A., Bernasconi S. M., Lilley M. D., Baross J. A., Summons R. E. and Sylva S. P. (2005) A serpentinite-hosted submarine ecosystem: the Lost City Hydrothermal Field. *Science* **307**, 1428–1434.

Kim S.-T., Hillaire-Marcel C. and Mucci A. (2006) Mechanisms of equilibrium and kinetic oxygen isotope effects in synthetic aragonite at 25 °C. *Geochim. Cosmochim. Acta* **70**, 5790–5801.

Klochko K., Kaufman A. J., Yao W., Byrne R. H. and Tossell J. A. (2006) Experimental measurement of boron isotope fractionation in seawater. *Earth Planet. Sci. Lett.* **248**, 261–270.

Lemarchand D., Gaillardet J., Lewin É. and Allègre C. J. (2002) Boron isotope systematics in large rivers: implications for the marine boron budget and paleo-pH reconstruction over the Cenozoic. *Chem. Geol.* **190**, 123–140.

Liu Y. and Tossell J. A. (2005) *Ab initio* molecular orbital calculations for boron isotope fractionations on boric acids and borates. *Geochim. Cosmochim. Acta* **69**, 3995–4006.

Ludwig K. A., Kelley D. S., Butterfield D. A., Nelson B. K. and Früh-Green G. (2006) Formation and evolution of carbonate chimneys at the Lost City Hydrothermal Field. *Geochim. Cosmochim. Acta* **70**, 3625–3645.

Massiot D., Fayon F., Capron C., King I., Le Calvé S., Alonso B., Durand J.-O., Bujoli B., Gan Z. and Hoatson G. (2002) Modelling one- and two-dimensional solid-state NMR spectra. *Magn. Reson. Chem.* **40**, 70–76.

McElligott S. and Byrne R. H. (1998) Interaction of $B(OH)_3^0$ and HCO_3^- in seawater: formation of $B(OH)_2CO_3^-$. *Aquat. Geochem.* **3**, 345–356.

Oi T. (2000a) Calculations of reduced partition function ratios of monomeric and dimeric boric acids and borates by the ab initio molecular orbital theory. *J. Nucl. Sci. Technol.* **37**, 166–172.

Oi T. (2000b) *Ab initio* molecular orbital calculations of reduced partition function ratios of polyboric acids and polyborate anions. *Z. Naturforsch.* **55a**, 623–628.

Oi T., Kato J., Ossaka T. and Kakihana H. (1991) Boron isotope fractionation accompanying boron mineral formation from aqueous boric acid–sodium hydroxide solutions at 25 °C. *Geochem. J.* **25**, 377–385.

Oi T. and Yanase S. (2001) Calculations of reduced partition function ratios of hydrated monoborate anion by the *ab initio* molecular orbital theory. *J. Nucl. Sci. Technol.* **38**, 429–432.

Pagani M., Lemarchand D., Spivack A. and Gaillardet J. (2005) A critical evaluation of the boron isotope-pH proxy: the accuracy of ancient ocean pH estimates. *Geochim. Cosmochim. Acta* **69**, 953–961.

Palmer M. R., Spivack A. J. and Edmond J. M. (1987) Temperature and pH controls over isotopic fractionation during adsorption of boron on marine clay. *Geochim. Cosmochim. Acta* **51**, 2319–2323.

Pearson P. N. and Palmer M. R. (1999) Middle Eocene seawater pH and atmospheric carbon dioxide concentrations. *Science* **284**, 1824–1826.

Pelejero C., Calvo E., McCulloch M. T., Marshall J. F., Cagan M. K., Lough J. M. and Opdyke B. N. (2005) Preindustrial to modern interdecadal variability in coral reef pH. *Science* **309**, 2204–2207.

Sanchez-Valle C., Reynard B., Daniel I., Lecuyer C., Martinez I. and Chervin J.-C. (2005) Boron isotopic fractionation between minerals and fluids: new insights from in situ high pressure-high temperature vibrational spectroscopic data. *Geochim. Cosmochim. Acta* **69**, 4301–4313.

Sanyal A., Bijma J., Spero H. J. and Lea D. W. (2001) Empirical relationship between pH and the boron isotopic composition of *G. sacculifer*: implications for the boron isotope paleo-pH proxy. *Paleoceanography* **16**, 515–519.

Sanyal A., Hemming N. G., Broecker W. S., Lea D. W., Spero H. J. and Hanson G. N. (1996) Oceanic pH control on the boron isotopic composition of foraminifera: evidence from culture experiments. *Paleoceanography* **11**, 513–517.

Sanyal A., Hemming N. G., Hanson G. N. and Broecker W. S. (1995) The pH of the glacial ocean as reconstructed from boron isotope measurements on foraminifera. *Nature* **373**, 234–236.

Sanyal A., Nugent M., Reeder R. J. and Bijma J. (2000) Seawater pH control on the boron isotopic composition of calcite: evidence from inorganic calcite precipitation experiments. *Geochim. Cosmochim. Acta* **64**, 1551–1555.

Sen S., Stebbins J. F., Hemming N. G. and Ghosh B. (1994) Coordination environments of boron impurities in calcite and aragonite polymorphs: an ^{11}B MAS NMR study. *Am. Mineral.* **79**, 818–825.

Sonoda A., Makita Y., Ooi K., Takagi N. and Hirotsu T. (2000) PH-dependence of the fractionation of boron isotopes with *N*-methyl-D-glucamine resin in aqueous solution systems. *Bull. Chem. Soc. Jpn.* **73**, 1131–1133.

Spivack A. J. and Edmond J. M. (1987) Boron isotope exchange between seawater and the oceanic crust. *Geochim. Cosmochim. Acta* **51**, 1033–1043.

Spivack A. J., You C. F. and Smith H. J. (1993) Foraminiferal boron isotope ratios as a proxy for surface ocean pH over the past 21 Myr. *Nature* **363**, 149–151.

Tossell J. A. (2006) Boric acid adsorption on humic acids: ab initio calculation of structures, stabilities, ^{11}B NMR and ^{11}B, ^{10}B isotopic fractionations of surface complexes. *Geochim. Cosmochim. Acta* **70**, 5089–5103.

Vengosh A., Kolodny Y., Starinsky A., Chivas A. R. and McCulloch M. T. (1991) Coprecipitation and isotopic fractionation of boron in modern biogenic carbonates. *Geochim. Cosmochim. Acta* **55**, 2901–2910.

Weiner S. and Dove P. M. (2003) An overview of biomineralization processes and the problem vital effect. *Rev. Mineral. Geochem.* **54**, 1–29.

Zeebe R. (2005) Stable boron isotope fractionation between dissolved $B(OH)_3$ and $B(OH)_4^-$. *Geochim. Cosmochim. Acta* **69**, 2753–2766.

Zeebe R. E., Wolf-Gladrow D. A., Bijma J. and Hönisch B. (2003) Vital effects in foraminifera do not compromise the use of $\delta^{11}B$ as a paleo-pH indicator: evidence from modeling. *Paleoceanography* **18**(2), 1043.

Associate editor: Alfonso Mucci